# Explosion at an intersection in an Urban Environment – Experiments and analyses

Morgan Johansson[a,*], Ola Pramm Larsen[b], and Leo Laine[b]

[a]REINERTSEN Sverige AB
Anders Carlssons gata 14, 417 55 Göteborg, Sweden
[*]Corresponding author: morgan.johansson@reinertsen.se

[b]ANKER – ZEMER Engineering A/S
P.O. Box 253, NO-0702 OSLO, Norway

This paper describes the experimental and numerical investigation of an explosion in an intersection built up of four concrete boxes. Scaled experiments (1:5) with a total of eight charges (0.4 and 1.6 kg) of PETN detonated at various locations and were registered using a total of 25 pressure gauges. The experimental results were used to validate numerical simulations made in the explicit code AUTODYN™ prior to the experimental performance. An automatic remapping procedure used in the simulations is briefly described and a coherence measure to compare experimental and numerical results is introduced. It is concluded that AUTODYN managed very well to predict the blast load obtained in a complex urban environment.

## INTRODUCTION

The Swedish Rescue Services Agency (SRSA) is responsible for the building regulations of the Swedish civil defence shelters. The shelters have specific regulations for how they are planned, built, equipped and maintained [1]. It is also the responsibility of SRSA to maintain and develop the knowledge connected to these structures. Based on this it has been concluded that there is a need to increase knowledge about the origin of blast loads and how they affect their surroundings. Accordingly, a research project, *Resistance capacities of buildings for extreme dynamic loading* [2], was initiated in 2006 wherein the main aim is to increase the knowledge of how to determine the capacity of any given building or group of buildings to withstand the effect of a blast load. This work is divided into two stages: determination of the load characteristics resulting from the blast load and development of a method to be used to estimate the capacity of a building subjected to such loads. This paper is part of the first stage.

Predicting the load caused by a propagating blast wave in urban environment, in which phenomena such as reflection, diffraction and confinement are to be taken into account, is a complex task. Remennikov [3] lists three types of methods to be used: empirical (or analytical), semi-empirical and numerical methods. For non-complex load cases it is usually sufficient to use engineering tools based on empirical data, e.g. ConWep [4]. For somewhat more complex geometry, though, it is necessary to use semi-empirical methods, i.e. methods based on models in which the important physical process is accounted for in a simplified way. Several researchers have also developed such models, e.g. [5]-[9], that work well within given limits and that provide an increased understanding of the resulting blast load. However, when the geometry gets more complex, which might be the case in an urban environment, it may no longer be possible to use such simplified tools, [10].

In such cases numerical methods incorporating computational fluid dynamics (CFD) techniques, so-called hydrocodes, may be used. However, even though the computational possibilities, regarding both the complexity of the analysis and the required computer time, steadily increase, it is still of utmost importance to make sure that the results obtained in such methods are correct. Hence, there is a need to verify such programs against experimental results. Once this is guaranteed it is possible to use hydrocode programmes to at least in part replace expensive experimental performances.

In this project the explicit code AUTODYN$^{TM}$ [11] is used and it has been shown in [12] that it provides satisfactory agreement with ConWep in analyses of spherical air bursts. However, it was necessary to verify that this also is the case in a more complex urban environment. Accordingly, an experimental test-series was conducted in co-operation between the Swedish Rescue Services Agency, the Norwegian Defence Estates Agency and the Swedish Defence Research Agency. The aim of this project is twofold: to increase the knowledge about blast load in a complex environment and to investigate the possibility for AUTODYN to predict the resulting load characteristics obtained in a complex environment.

The outline of the paper is as follows: The section EXPERIMENTAL SETUP show how the experiments were performed. The section FINITE ELEMENT MODEL discuss how the model was set-up and what material properties were used for the explosive and air. In the RESULTS section analyses are carried out and results are shown. Finally CONCLUSIONS summarises the findings.

## EXPERIMENTAL SETUP

The experimental location consisted of four concrete cubic boxes (dimension 2.3 m) positioned at a distance of 2.3 m apart. Three types of charges, 0.4 kg PETN, 1.6 kg PETN and 1.6 kg TBX, were used and positioned either close to the ground (0.20 m) or at mid height (1.15 m) of the concrete boxes in four different locations, see Fig. 1. The tests were carried out in scale 1:5 meaning that the concrete boxes approximately corresponded to a four-storey building of height 11.5 m with a small charge of 50 kg pentolite, detonating 1.0 m above ground; i.e. a threat situation roughly equal to what might be expected from a small car bomb.

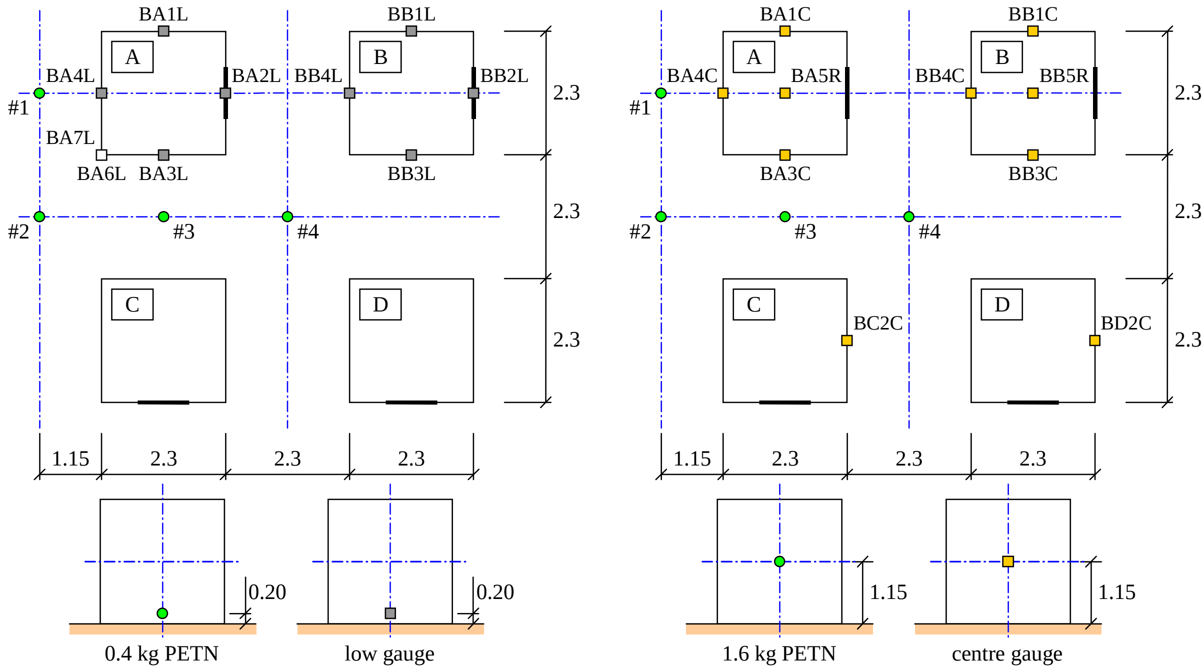


Fig. 1. Top view of the experimental set-up and gauges located on the concrete boxes. The charges were placed in four different positions (#1 – #4) 0.2 m (0.4 kg PETN) or 1.15 m (1.6 kg PETN) above the ground. The naming of the gauges is as follows: Building letter, Gauge no., Low or Centre. All lengths are in metres.

A total of 25 pressure gauges were used to register the pressure-time relations at various locations. 20 gauges (brand: Kulite) had fixed positions in the concrete boxes: 10 low (L) at a level of 0.20 m, 8 in the centre (C) at 1.15 m above the ground and 2 on the roof (R), see Fig. 1. All gauges but two were positioned in the middle of the wall/roof. The last two gauges (BA6L and BA7L) were positioned close to the ground 0.20 m from one of the wall edges in an attempt to get an approximate reading of the effect the diffraction has on the pressure. The remaining 5 gauges (brand: PCB) were fastened on wooden boards placed on the ground and had various positions according to Fig. 2, depending on the position of the charge. Even though all gauges were active in every detonation those gauges set low and in the centre were mainly used for the evaluation of 0.4 kg and 1.6 kg charges, respectively.

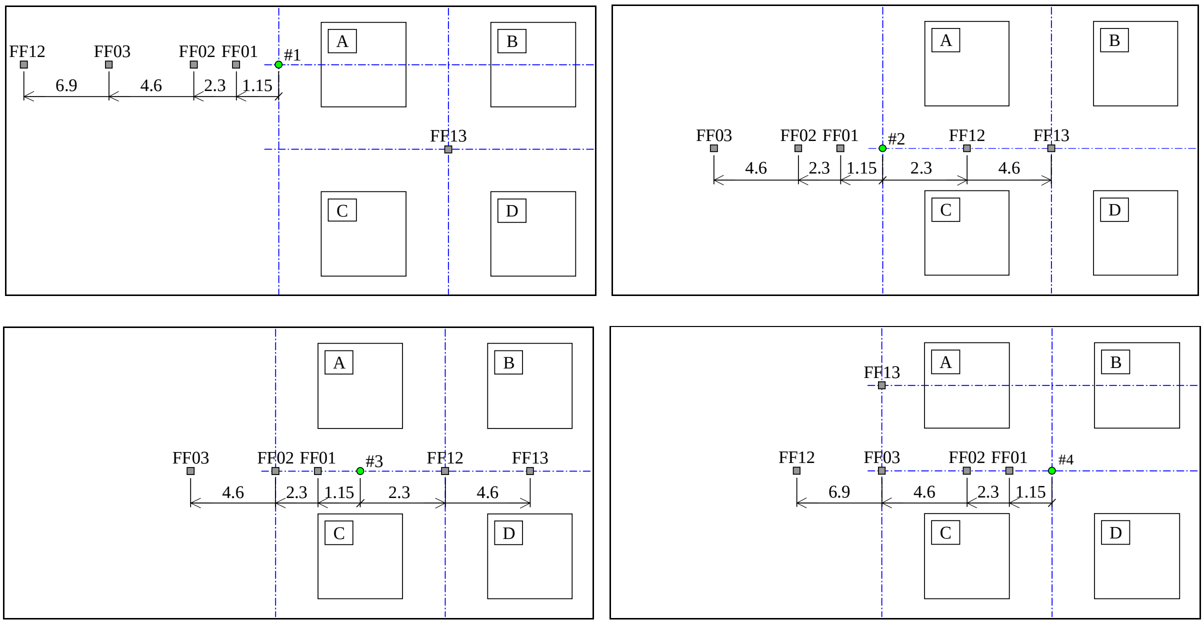


Fig. 2. Top view of the different ground pressure gauge positioning for each charge location. All lengths are in metres.

The explosive used was the Swedish PETN, Sprängdeg m/46, with a density of about 1 500 kg/m$^3$, which consists of approximately 86 % pentolite and 14 % mineral oil. Accordingly, the 0.4 kg and 1.6 kg charges used consisted of 0.344 kg and 1.376 kg pentolite, respectively. In ConWep [2] the equivalent weight (compared to TNT) of pentolite is given as 1.42 kg and 1.00 kg for pressure and impulse, respectively. However, when determining the pressure-time relations for pentolite ConWep uses the average of these values, i.e. 1.21 kg, and accordingly, a charge of 1 kg Sprängdeg m/46 corresponds to $0.86 \cdot 1.21 \approx 1.04$ kg TNT. Using this correlation an approximate value of the scaled distance $Z = R/W^{1/3}$ can be determined. The horizontal projection of the distance between the charges and the pressure gauges varied from 1.15 m to about 10 m; resulting in $1.5 \leq Z \leq 13$ m/kg$^{1/3}$ and $1.0 \leq Z \leq 8.5$ m/kg/$^{1/3}$ for the 0.4 kg and 1.6 kg charge, respectively.

In this paper only the results for PETN charges, and then mainly those caused by the smaller 0.4 kg charges, are presented. For more detailed information about the experiments and the analyses performed, see [13].

## FINITE ELEMENT MODEL

The blast simulations were performed using the explicit code AUTODYN [11]. All simulations were made before the experiments were carried out, which means that the experimental results are used to validate how well AUTODYN manage to describe the blast load in a complex environment similar to that in a city.

In the numerical model the physical domain was represented by rectangular boxes in 3D which in turn were filled with cube shaped hexahedral linear elements. The size of these rectangular boxes varied based on the blast scenarios as well as the different remap stages and the planar symmetry present. A typical series of 3D remap runs over 4 stages would have approximate rectangular domain sizes of: $(2\ m)^3$, $(4\ m)^3$, $(8\ m)^3$ and $(16\ m)^3$. The element size used highly depended on the remap stage and the total number of elements employed in the numerical mesh. The high resolution runs strived to utilise the maximum number of elements possible under the 32 bit addressing space providing approximately 4.5 million elements, which in turn yielded an element size of approximately 10 mm at the first 3D remap stage. The remapping ratio was always 1:2, consequently doubling the element size in each direction at every new remap stage. The four concrete blocks and the ground were modelled using rigid boundaries. The outflow boundary condition was only applied during the last 3D remapping stage to the external phases of the domain. At all other stages no boundary conditions were necessary since the blast wave front was always fully contained inside the corresponding numerical domain.

Each simulation involved separate runs over several stages in which a self-developed automatic remapping technique, further discussed below, was used. The first stage involved a 1D spherical symmetric run using a Multi-Material Euler solver simulating the initial detonation phase with both explosive material and air. A remap procedure was then performed into a 2D axial symmetric domain using the same Multi-Material Euler solver. Finally the simulation was concluded by a series of 3D remapping runs using an Euler-FCT solver with air only. Some of these 3D remapping stages involved planar symmetry, in which case the symmetry was fully exploited in the simulations. All of the eight blast scenarios were completed with as many as 7-9 AUTODYN simulations employing different mesh resolutions for quality assurance and convergence studies. Fig. 3 illustrates the simulation procedure over the various 3D remapping stages.

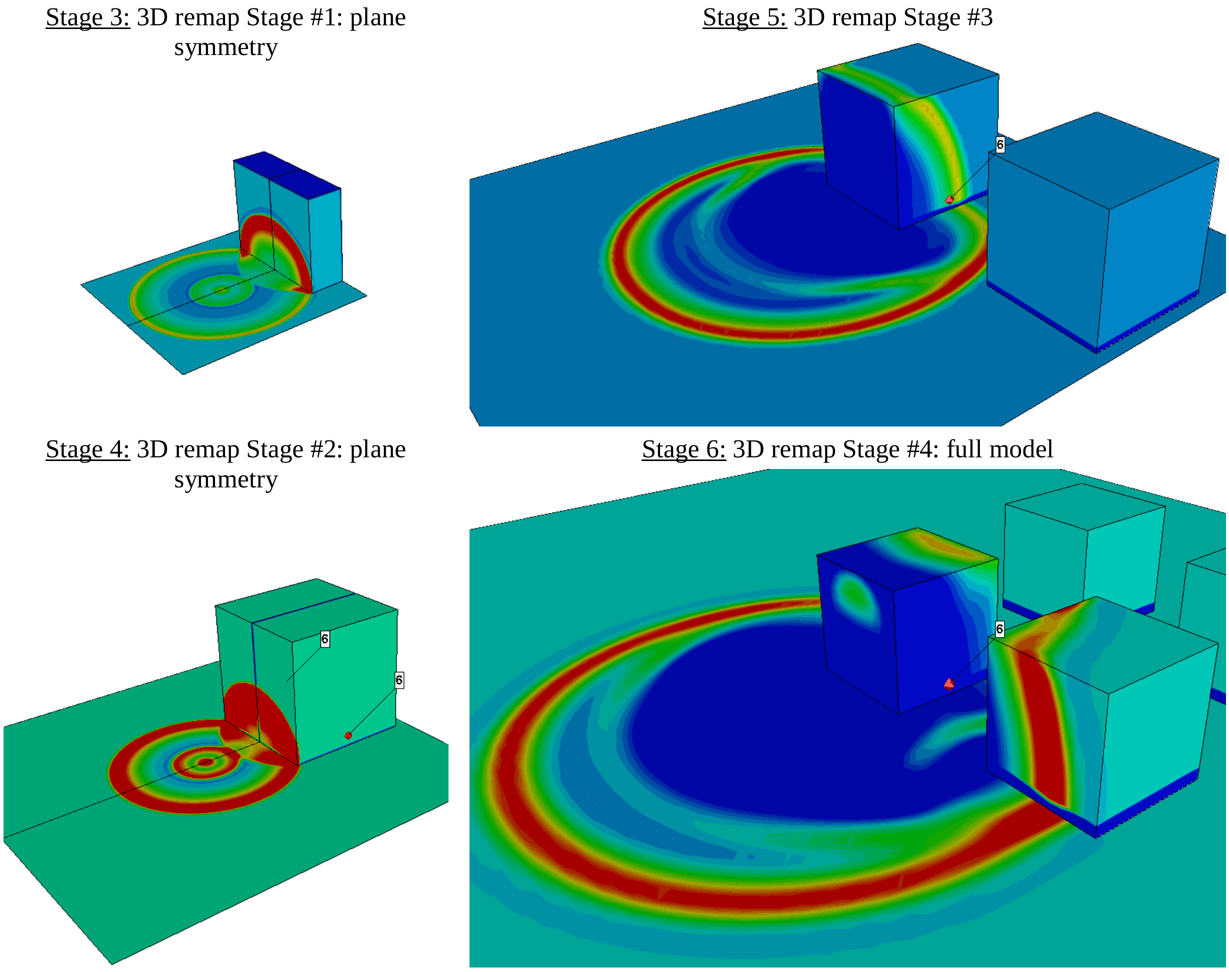


Fig. 3. Illustration of the principal layout of the finite element model for simulation of charge at location #1 for Stages 3 to 6: 3D stages using automatic remapping. Stage 1 (1D spherical symmetry) and Stage 2 (2D axial symmetry) are not shown.

The vast number of simulations with their accompanying remapping stages performed in this project called for automation at several levels of the simulation process. A quite complex system integrating automatic script generation with AUTODYN-linked Fortran user-subroutines were therefore developed. This automation system enabled the batch simulation run of an unlimited number of 3D blast scenarios, each containing several remap stages with arbitrary geometry and symmetry conditions, with a click of a button. The main idea of this methodology is to enable automatic detection of the shock front during the blast, so that a remap process can be initiated at the time when the shock front is close to the boundary. The global script file controls the whole process from the generation of the new remapped FE models up to the batch control of several simulations running in series.

In AUTODYN there are four different pre-defined material models for the explosive PETN, where the material densities are set to: 0.88 kg/m$^3$, 1.26kg/m$^3$, 1.50 kg/m$^3$ and 1.77 kg/m$^3$. Which model should be used was unclear, and therefore, an investigation of the different material models were carried out in order to find out what pressures and impulse intensities could be expected for different values of the scaled distance $Z = R/W^{1/3}$. This was done in AUTODYN using a one-dimensional wedge analysis simulating an undisturbed spherical pressure release. The results were compared with a corresponding analysis of TNT, [12], and are for the overpressure summarised in Fig. 4. Here the overpressure is presented as a function of the scaled distance and based on this the equivalent weight of TNT was determined. From this it can be seen that the resulting pressure will be almost identical for the PETN material models, with densities 1.26 kg/m$^3$ and higher, available in AUTODYN. It can also be concluded that the equivalent weight, based on the average value for $2 \leq Z \leq 10$ m/kg$^{1/3}$, is about 1.45 kg for the pressure. The corresponding relation for the impulse intensity was determined as well and was found to be very similar with the same average equivalent weight of 1.45 kg. Comparing these values with those given in ConWep – 1.42 kg for pressure and 1.00 kg for impulse – shows that the equivalent weight based on pressure was very similar but that it differed considerably for the impulse intensity.

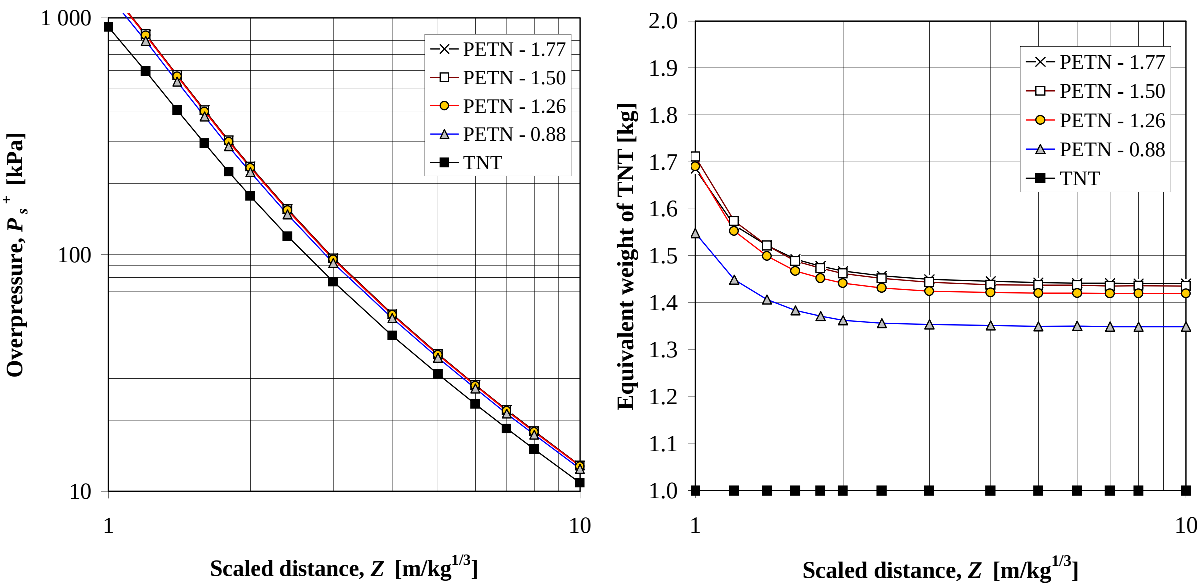


Fig. 4. Results obtained for different explosive PETN material models in AUTODYN: Pressure as function of scaled distance (left) expressed as corresponding equivalent weight of TNT (right).

Based on the above and an approximation that the explosive in the charges used had a density of about 1.7 kg/m$^3$, [13], the PETN material model with density 1.77 kg/m$^3$ was used in the final AUTODYN simulations of the experimental set-up. The explosive was modelled using the JWL Equation of State (EOS) with automatic conversion into Ideal Gas EOS when the entire explosive had reached a compression value of -0.95. Furthermore, at the start of the first 3D remap stage the explosive was converted into air, thus facilitating the use of the single material Ideal-Gas-EOS-Only Euler FCT solver. Input parameters for air and explosive are listed in Table 1.

Table 1. Summary of input parameters in AUTODYN for air and explosive PETN with density 1.77 kg/m$^3$.

| **Air** | |
|---|---|
| $\rho_0$ | $1.226 \cdot 10^{-3}$ (g/cm$^3$) |
| $\gamma$ | 1.4 |
| $P_0$ | 101.3 (kPa) |

| **PETN 1.77** | |
|---|---|
| $\rho_0$ | 1.77 (g/cm$^3$) |
| C-J Detonation velocity | 8 300 (m/s) |
| C-J Energy density | $1.01 \cdot 10^7$ (kJ/m$^3$) |
| C-J Pressure | $3.35 \cdot 10^7$ (kPa) |

## RESULTS

Most of the ground pressure gauges (FF01 to FF13) were positioned within a straight line free from obstructions from the charge, see Fig. 2, meaning that a direct comparison with results from ConWep is possible. In Fig. 5 the peak pressures, registered in the ground gauges for different charge locations in the experiments, are compared to that of ConWep. The correspondence is fairly good for the short distances of 1.15 m and 2.3 m while it is less accurate for the longer distances of 4.6 m and 6.9 m. This difference is partly due to the confinement effect that the concrete boxes present (especially true for the charge at location #4) but can not fully explain the difference observed. It should be noted, though, that the peak pressure might be a bit difficult to capture properly and that the impulse intensity is a more reliable measure for this type of comparison. However, the disturbances caused by the surrounding concrete boxes, i.e. confinement and reflection effects, make such a comparison with ConWep irrelevant. Nevertheless, the results are regarded to be sufficiently close to ConWep to be satisfactory and more detailed information of resulting pressure-time relations from the experiments are presented together with the numerical analyses below.

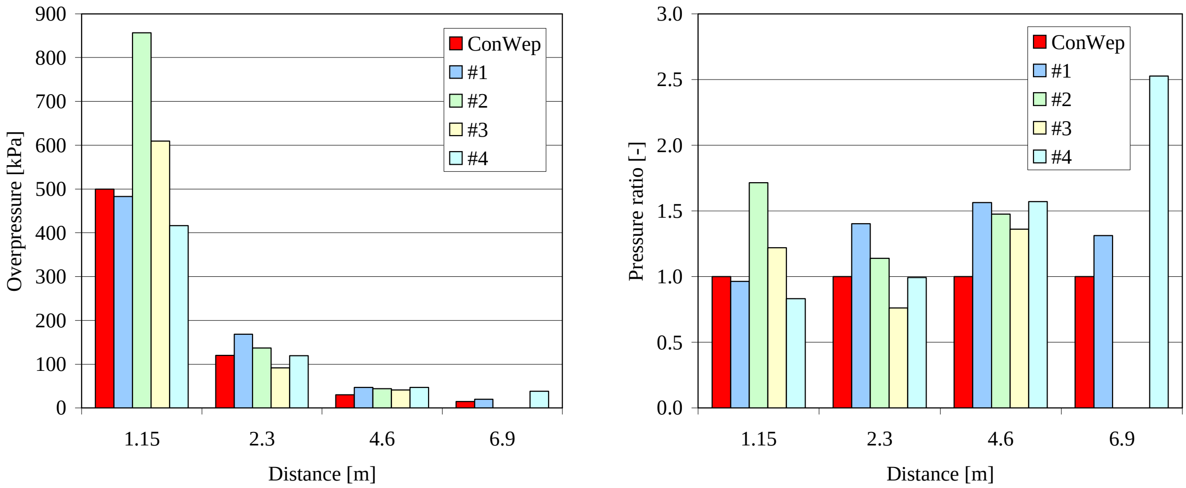


Fig. 5. Comparison of overpressures obtained at ground pressure gauges (FF01 to FF13 in Fig. 2) in experiments and ConWep. The left diagram shows the incident overpressures while the right shows these pressures expressed as a ratio of the peak pressure obtained in ConWep. The deviation observed for charge at location #4 is expected due to confinement effects.

Table 2 presents a comparison of key parameters overpressure $P^+$, arrival time $t_a$ and impulse intensity $i^+$ and $i^-$ obtained in the AUTODYN simulations and that of the experiments. Here, the impulse intensity is defined as the sum of all positive and negative phases, respectively, within the time period $t_{end}$ as shown in Eqs. (1) and (2).

$$i^+ = \sum_{k=1}^{n} i_k^+ = \sum_{k=1}^{n} \int_{t_{k,a}}^{t_{k,end}} P^+(t)dt \qquad (1)$$

$$i^- = \sum_{k=1}^{n} i_k^- = \sum_{k=1}^{n} \int_{t_{k,a}}^{t_{k,end}} P^-(t)dt \qquad (2)$$

Table 2. Summary of key parameters $P^+$, $t_a$, $i^+$ and $i^-$ from AUTODYN analyses and experiments. The impulse intensities $i^+$ and $i^-$ are determined according to Eq. (1) and Eq. (2) with $t_{end}$ = 50 ms. A “-“ in the table indicate that the experimental result was not valid.

| | Location #1 | | | | | | | | Location #2 | | | | | | | |
|---|---|---|---|---|---|---|---|---|---|---|---|---|---|---|---|---|
| Gauge | AUTODYN | | | | Experiments | | | | AUTODYN | | | | Experiments | | | |
| | $P^+$ [kPa] | $t_a$ [ms] | $i^+$ [Pas] | $i^-$ [Pas] | $P^+$ [kPa] | $t_a$ [ms] | $i^+$ [Pas] | $i^-$ [Pas] | $P^+$ [kPa] | $t_a$ [ms] | $i^+$ [Pas] | $i^-$ [Pas] | $P^+$ [kPa] | $t_a$ [ms] | $i^+$ [Pas] | $i^-$ [Pas] |
| FF01 | 656 | 0.62 | 143 | 137 | 480 | 0.65 | 248 | - | 755 | 0.61 | 155 | 152 | 859 | 0.46 | 240 | 160 |
| FF02 | 129 | 2.42 | 85 | 94 | 168 | 2.58 | 57 | - | 137 | 2.41 | 86 | 98 | 161 | 2.22 | 77 | 97 |
| FF03 | 32 | 7.69 | 52 | 50 | 47 | 8.14 | 82 | 54 | 33 | 7.72 | 50 | 51 | 41 | 7.89 | 51 | 41 |
| FF12 | 14 | 13.45 | 35 | 35 | 20 | 14.27 | 38 | 35 | 140 | 2.36 | 167 | 168 | 111 | 2.52 | 150 | 192 |
| FF13 | 16 | 9.89 | 32 | 32 | 18 | 10.50 | 28 | 31 | 52 | 7.62 | 74 | 72 | 47 | 8.03 | 70 | 80 |
| BA1L | 51 | 3.71 | 61 | 67 | - | - | - | - | 12 | 7.94 | 35 | 37 | 11 | 8.00 | 33 | 35 |
| BA2L | 7 | 9.63 | 49 | 48 | 8 | 10.28 | 53 | 49 | 12 | 7.94 | 62 | 63 | 12 | 8.50 | 60 | 62 |
| BA3L | 51 | 3.71 | 113 | 115 | 63 | 3.89 | 112 | 110 | 233 | 2.82 | 165 | 159 | 271 | 2.90 | 190 | 176 |
| BA4L | 2 100 | 0.63 | 461 | 208 | 1 745 | 0.63 | 429 | - | 233 | 2.82 | 127 | 126 | 155 | 2.96 | 93 | 116 |
| BA6L | 94 | 1.56 | 76 | 148 | 114 | 1.68 | 104 | 107 | 470 | 1.43 | 206 | 173 | - | - | - | - |
| BA7L | 1 221 | 1.05 | 290 | 211 | 599 | 1.02 | 187 | 452 | 470 | 1.43 | 192 | 159 | 373 | 1.46 | 159 | 134 |
| BB1L | 6 | 15.34 | 20 | 22 | 11 | 16.76 | 22 | 19 | 4 | 16.59 | 21 | 22 | 6 | 17.72 | 21 | 21 |
| BB2L | 3 | 22.00 | 21 | 20 | 3 | 23.35 | 23 | 20 | 4 | 19.46 | 15 | 15 | 4 | 20.62 | 16 | 15 |
| BB3L | 6 | 15.34 | 42 | 44 | 11 | 16.63 | 45 | 44 | 24 | 13.31 | 59 | 60 | 30 | 14.17 | 60 | 61 |
| BB4L | 14 | 13.41 | 68 | 70 | - | - | - | - | 26 | 11.76 | 69 | 63 | 26 | 12.23 | 67 | 62 |
| | Location #3 | | | | | | | | Location #4 | | | | | | | |
| Gauge | AUTODYN | | | | Experiments | | | | AUTODYN | | | | Experiments | | | |
| FF01 | 698 | 0.62 | 226 | 184 | 610 | 0.61 | 237 | 704 | 755 | 0.61 | 177 | 176 | 431 | 0.56 | 168 | 210 |
| FF02 | 136 | 2.38 | 140 | 141 | 93 | 2.53 | 120 | 220 | 142 | 2.38 | 152 | 160 | 119 | 2.43 | 141 | 167 |
| FF03 | 33 | 7.74 | 76 | 77 | 45 | 7.78 | 71 | 66 | 50 | 7.64 | 73 | 71 | 47 | 8.02 | 54 | 118 |
| FF12 | 136 | 2.38 | 137 | 141 | 93 | 2.63 | 113 | 155 | 25 | 13.35 | 42 | 42 | 38 | 13.73 | 40 | 41 |
| FF13 | 34 | 7.61 | 114 | 112 | 37 | 8.21 | 106 | 102 | 13 | 9.28 | 34 | 35 | 14 | 9.63 | 35 | 28 |
| BA1L | 8 | 9.71 | 52 | 51 | 8 | 9.81 | 49 | 47 | 13 | 7.99 | 35 | 35 | 12 | 8.39 | 32 | 31 |
| BA2L | 52 | 3.73 | 113 | 115 | 40 | 3.90 | 110 | 116 | 234 | 2.83 | 155 | 154 | 110 | 2.90 | 126 | 147 |
| BA3L | 2 258 | 0.63 | 505 | 235 | 2 369 | 0.47 | 763 | 328 | 234 | 2.83 | 154 | 153 | 238 | 3.00 | 131 | 191 |
| BA4L | 52 | 3.73 | 70 | 73 | 58 | 3.81 | 73 | 74 | 13 | 7.99 | 35 | 35 | 11 | 8.45 | 32 | 31 |
| BA6L | 1 272 | 1.05 | 325 | 233 | 991 | 1.03 | 345 | 238 | 113 | 4.66 | 126 | 125 | 113 | 4.81 | 118 | 130 |
| BA7L | 103 | 1.61 | 70 | 132 | 146 | 1.65 | 72 | 174 | 22 | 5.48 | 47 | 59 | 34 | 5.84 | 52 | 60 |
| BB1L | 8 | 11.55 | 34 | 31 | 8 | 12.34 | 32 | 27 | 13 | 7.99 | 35 | 35 | 12 | 8.12 | 33 | 31 |
| BB2L | 5 | 13.52 | 33 | 35 | 5 | 13.85 | 32 | 33 | 13 | 7.99 | 35 | 35 | 12 | 7.62 | 37 | 35 |
| BB3L | 51 | 7.93 | 115 | 112 | 54 | 8.39 | 99 | 98 | 234 | 2.83 | 154 | 153 | 143 | 2.87 | 124 | 144 |
| BB4L | 77 | 6.45 | 131 | 127 | 73 | 6.89 | 122 | 118 | 234 | 2.83 | 155 | 154 | 124 | 2.86 | 127 | 151 |

From this summary it is also clear that the correspondence between experiments and AUTIDYN simulations in several cases are very good. However, to get a better picture of how well the results coincide a coherence measure, according to Eq. (3), was introduced.

$$Coh = 1 - \frac{\int_{t_a}^{t_{end}} \left| P_{AD}(t) - P_{Exp}(t) \right| dt}{i_{Exp}^{+} + i_{Exp}^{-}} \qquad (3)$$

Here $P_{AD}(t)$ and $P_{Exp}(t)$ are the pressure obtained in the AUTODYN simulations and experiments, respectively, while $i^+_{Exp}$ and $i^-_{Exp}$ are the total positive and negative impulse intensities from the experiments during the time interval $t_a \leq t \leq t_{end}$. Thereby, it is possible to fairly straightforwardly compare a large number of numerical and experimental results and get a measure of how well they coincide. In Eq. (3) $Coh$ = 1.0 signify a perfect match. However, in general a coherence value of 0.5 or better corresponds to very good agreement between simulated and experimental results, see Fig. 6.

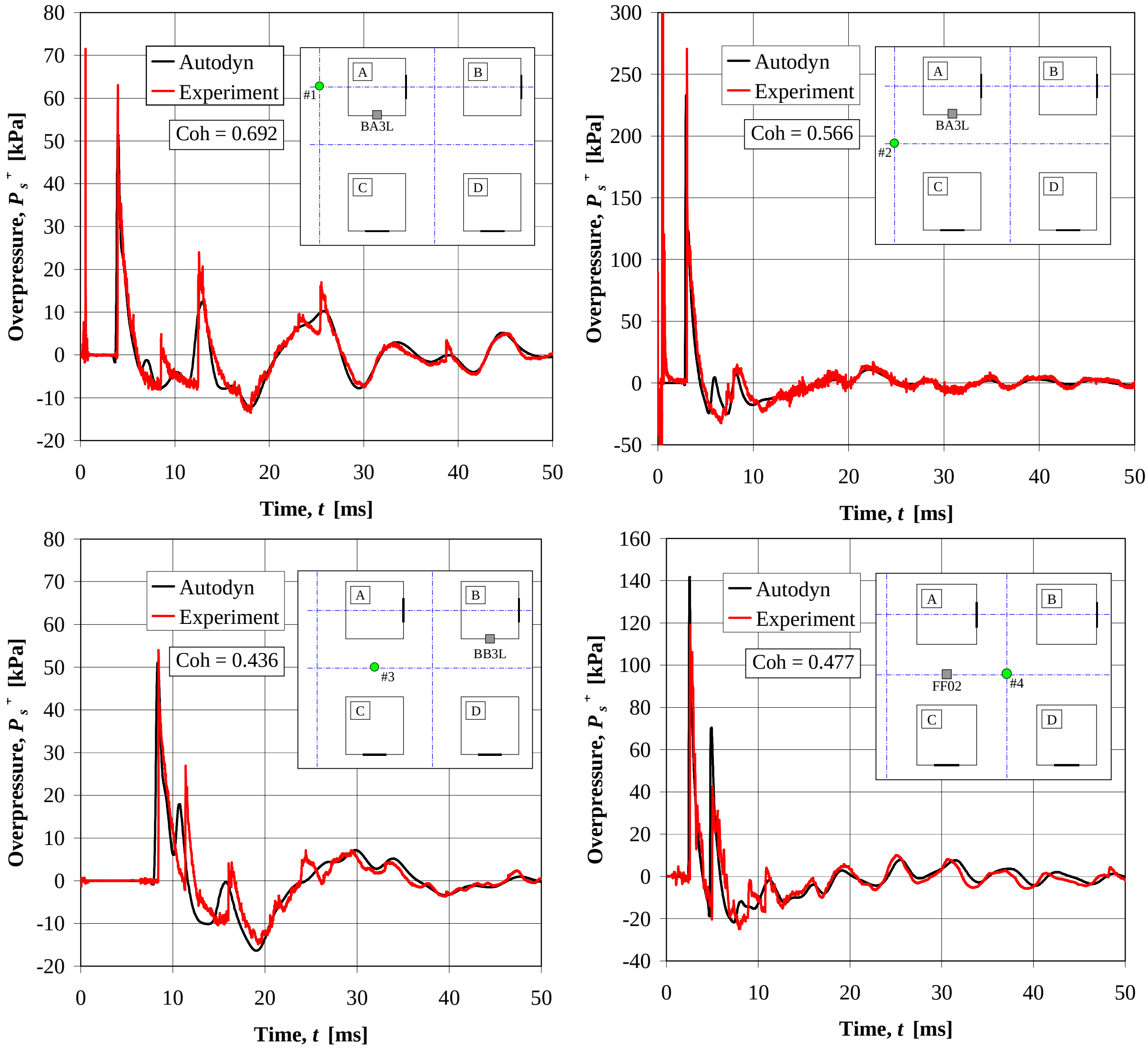


Fig. 6. Example of correlation between AUTODYN analyses and experiments: charge location #1, gauge BA3L (top left); charge location #2, gauge BA3L (top right); charge location #3, gauge BB3L (bottom left) and charge location #4, gauge FF02. The coherences are 0.692, 0.566, 0.436 and 0.477, respectively.

From Table 2 and Fig. 6 it can be seen that the agreement between experimental and numerical results are generally very good. Even though it can be concluded that most results coincided well it was generally observed that the agreement between analyses and experimental results increased when the peak pressure decreased. Thus, when the pressure reduces to less than about 50-100 kPa the general agreement went from very good to excellent. In Fig. 7 the complete batch of coherence data for the 0.4 kg and 1.6 kg charges, totalling 8 charges with almost 200 result series (all in all about 10 gauges failed to produce any trustworthy results during the experiments), is presented. The results have been separated into two groups, 0.4 kg and 1.6 kg charges, and it can be seen that the coherence generally is somewhat higher for the larger charges. Further, it can be noted that about 65 % of the compared results reach a coherence of 0.5 or higher; i.e. a limit indicating very good agreement.

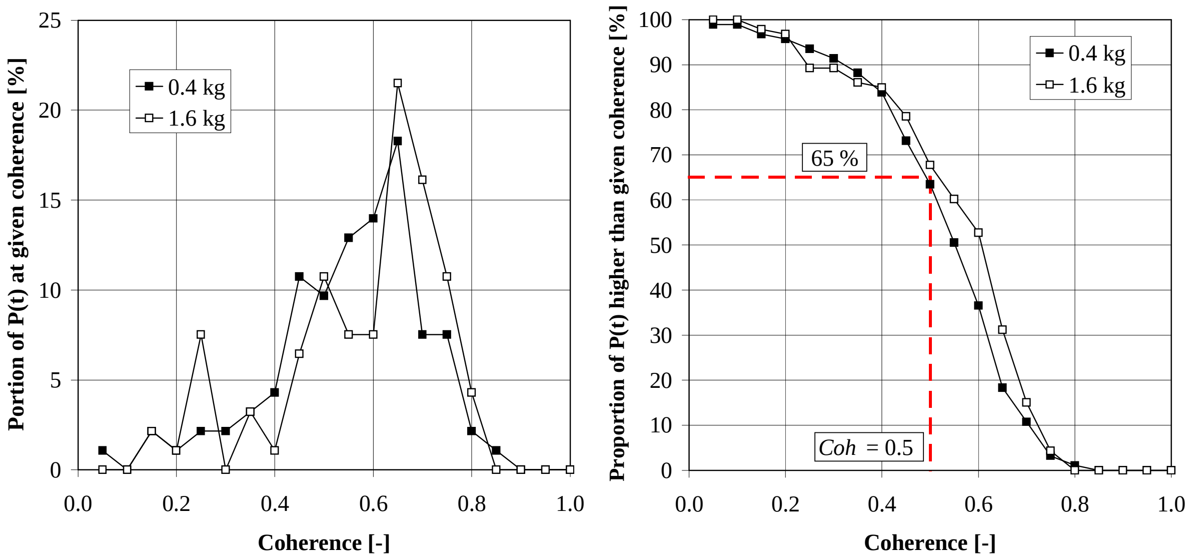


Fig. 7. Coherence of 0.4 kg and 1.6 kg charges presented as portion at given coherence (left) and portion higher than given coherence (right). A coherence value of about 0.5 or higher corresponds to very good agreement, see Fig. 6, and this limit is reached by approximately 65 % of the compared results.

## CONCLUSIONS

An experimental and numerical study of blast load at an intersection has been carried out. The load effects of two types of charges, 0.4 kg and 1.6 kg PETN, positioned in four different locations have been simulated using the explicit code AUTODYN and compared to the experimental results. It shall be pointed out that all AUTODYN analyses were made before the experiments were carried out. Hence, the results presented herein are used to validate how well AUTODYN manage to describe the blast behaviour in a complex geometry such as in a city environment.

In the blast simulations in AUTODYN an automatic remapping routine is introduced. This routine enabled automatic detection of the shock front close to a boundary, and thus a criterion for when, in time, to initiate the remapping process. Consequently, an automatic remapping of the modelled volume is possible, allowing for a more simplified approach to large blast simulations in a complex environment.

It is shown that there generally is very good agreement between the results obtained in the experiments and the AUTODYN simulations. A coherence measure is introduced for comparing experimental and numerical results and it is concluded that this is a convenient method to get a rough estimation of how well the results coincide. It is shown that for the results presented herein a measure of $Coh \geq 0.5$ signify very good agreement and that about 65 % of the compared measurements fulfil this limit. For gauges where the pressure was low (less than about 50-100 kPa) the agreement went from very good to excellent. Consequently, it is concluded that AUTODYN manage very well to describe the resulting blast effects in a complex city environment.

As a sub result of this study the relations for pressure and impulse intensity for the four PETN explosives, predefined in AUTODYN, are presented and it is shown that there is only a minor difference between three of them. It is also shown that the equivalent weight, compared to TNT, is about 1.45 kg for both pressure and impulse for scaled distances of $2 \leq Z \leq 10$ m/kg$^{1/3}$; which differ to what is stated in e.g. ConWep.

Even though it is shown herein that AUTODYN performed very well in its prediction of the load characteristics obtained in the experiments, it shall be pointed out that empirical and semi-empirical methods still fulfil an important task in that they provide a basic explanation necessary for understanding complex load situations. Accordingly, such less complex methods are still necessary to better understand the results from a CFD analysis, and hence help prevent the latter from being transformed into a “black box”. It would even be beneficial to use a combination of numerical simulations and experimental data to further improve and develop semi-empirical models in order to better understand the blast load obtained in complex urban environments.

## ACKNOWLEDGEMENTS

The authors thankfully acknowledge the support given by the Swedish Rescue Services Agency and especially Björn Ekengren for their support in the project. Furthermore we would like to thank the Norwegian Defence Estates Agency and the Swedish Defence Research Agency for their initiation and successful co-operation with the experimental work presented herein.

## REFERENCES

[1] Ekengren B., 2006, Skyddsrum, SR 06, Swedish Rescue Services Agency, B54-141/06, Karlstad, Sweden.

[2] Johansson, M. and Laine., L., *Resistance capacities of buildings for extreme dynamic loading,* Research project description, Swedish Rescue Services Agency, http://www.srv.se/templates/SRV_Page____15919.aspx, Karlstad, Sweden.

[3] Remennikov, A.M., "A review of methods for predicting bomb blast effects on buildings," Journal of Battlefield Technology, 2003, 6(3), pp. 5–10.

[4] ConWep, 1992, ConWep – Collection of conventional weapons effects calculations based on TM 5-855-1, Fundamentals of Protective Design for Conventional Weapons, U.S. Army Engineer Waterways Experiment Station, Vicksburg, USA.

[5] Rose, T.A. and Smith, P.D., "Influence of the principal geometrical parameters of straight city streets on positive and negative phase blast wave impulses," *International Journal of Impact Engineering*, 2002, 27, pp. 359–376.

[6] Rose, T.A. and Smith, P.D., "The influence of street junctions on blast wave impulses produced by vehicle bombs, "*Proceedings of the 11th International Symposium on Interaction of the Effects of Munitions with Structures*, 2003, Mannheim, Germany.

[7] Dörr, A., Brombacher, B., Gürke, G., "Blast behind street junctions originating from vehicle bombs," *Proceedings of 18th Symposium on the Military Aspects of Blast and Shock*, 2004, Bad Reichenhall, Germany.

[8] von Rosen, B., Guilbeault, E., Contesabile, E., "A preliminary investigation into the interaction of shock waves behind a simple rectangular structure," *Proceedings of 18th Symposium on the Military Aspects of Blast and Shock*, 2004, Bad Reichenhall, Germany.

[9] Remennikov, A.M. and Rose, T.A., "Modelling blast loads on buildings in complex city geometries," *Computers and Structures*, 2005, 83, pp. 2197-2205.

[10] Smith, P.D. and Rose, T.A., "Blast wave propagation in city streets – an overview," *Prog. Struct. Engng Mater*. 2006, 8, pp. 16-28.

[11] Century Dynamics Inc., 2004, AUTODYN Theory Manual Revision 5.0, San Ramon, CA, USA.

[12] Johansson, M. and Laine, L., 2007, "Bebyggelsens motståndsförmåga mot extrem dynamisk belastning, Delrapport 1: Last av luftstötvåg" ("Resistance capacities of buildings for extreme dynamic loading, Report 1: Load from airblast", in Swedish.), Swedish Rescue Services Agency, B54-232/07, Karlstad, Sweden.

[13] Johansson, M. and Laine, L., 2008, "Bebyggelsens motståndsförmåga mot extrem dynamisk belastning, Delrapport 2: Explosion i gatukorsning" ("Resistance capacities of buildings for extreme dynamic loading, Report 2: Explosion at an intersection", in Swedish.), Swedish Rescue Services Agency, to be published in 2008, Karlstad, Sweden.